Available online at www.sciencedirect.com
SCIENCE DIRECT®
ELSEVIER
Optical Materials 27 (2005) 763–768
OPTICAL Materials
www.elsevier.com/locate/optmat

Birefringence characterization of mono-dispersed silicon nanocrystals planar waveguides

D. Navarro-Urrios [a,*], F. Riboli [a], Massimo Cazzanelli [a], A. Chiasera [a], N. Daldosso [a], L. Pavesi [a], C.J. Oton [b], J. Heitmann [c], L.X. Yi [c], R. Scholz [c], M. Zacharias [c]

[a] *Dipartimento di Fisica, Università di Trento, via Sommarive 14, I-38050 Povo, Trento, Italy*
[b] *Departamento de Física Básica, University of La Laguna, Avda. Astrofísico Fco. Sánchez, La Laguna 38204, Spain*
[c] *Institute of Microstructure Physics, Weinberg 2, 06120 Halle, Germany*

Available online 8 October 2004

Abstract

In this work, we present the waveguiding properties of a set of mono-dispersed silicon nanocrystal Si-nc superlattices. The measured modal refractive indices (obtained by the m-line technique) of different samples can only be explained by assuming a negative "form birefringence" of about 1% originating from the particular structure of the active core, i.e., a periodical set of parallel planes of two different materials. By means of a simple model for the ordinary and extraordinary refractive indices in this kind of structures, by using the information from TEM images and the nominal growth parameters, and by considering as free parameters the upper size of the diameter of Si-nc, we are able to fit the m-line measurements in a unique way. We also report gain measurements on this set of samples, showing that, under high power pulsed excitation, positive optical gain is observed in samples that provide both good light confinement inside the waveguide and the right Si-nc dimension.
© 2004 Elsevier B.V. All rights reserved.

PACS: 78.20.Bh; 78.20.Fm; 78.67.Bf; 78.67.Pt

1. Introduction

Low dimensional silicon, as silicon nanocrystals (Si-nc), is a material with extremely interesting optoelectronic properties [1]. Efficient room temperature emission which can also be electrically excited [2] and non-linear optical properties with increased third order non-linear susceptibility [3] had been reported. The use of Si-nc is also one of the possible approaches to have a silicon laser operating at around 750 nm [4]. The experimental work in this field has raised up very rapidly with the aim to confirm or, independently, to demonstrate that stimulated emission from silicon is possible [5–9]. The lowering of the dimensionality of silicon in Si-nc, together with their interaction with the embedding matrix (usually SiO_2) are invoked to explain the high emission efficiency and the observation of net optical gain. The usual process to form Si-nc is by a thermally induced phase separation of Si and SiO_2. With this method an undesired result is the large size dispersion of the Si-nc, which causes an inhomogeneous broadening of the emission band and reduces stimulated emission efficiency. Recently an approach to reduce the size dispersion of Si-nc has been proposed [10] by using amorphous SiO_2/SiO_y ($y < 2$) superlattices. After thermal annealing at high temperature, a phase separation occurs only in the deposited SiO_y layers where Si-nc form with a typical size constrained to the SiO_y layer thickness. This leads to a stack of layers of SiO_2 and Si-nc rich SiO_2, named superlattice (SL) in the following, that shows narrow Si-nc size dispersion [10].

* Corresponding author. Tel.: +39 46 1882030; fax: +39 48 1881696.
E-mail address: navarro@science.unitn.it (D. Navarro-Urrios).

0925-3467/$ - see front matter © 2004 Elsevier B.V. All rights reserved.
doi:10.1016/j.optmat.2004.08.011

Because the Si-nc are much smaller than the wavelength of the light, this kind of samples has homogeneous optical properties. As we have already mentioned, in samples grown by the usual method, Si-nc are randomly arranged over the waveguide core, making the material refractive index to be isotropic. On the contrary, in a Si-nc SL which is made by two alternative materials with different refractive indices, the optical behaviour is no more isotropic. The light polarized parallel to the layers (TE-polarization) experiments the ordinary refractive index (n_o), which is higher than the extraordinary refractive index (n_e) experimented by the light polarized perpendicularly to the layers (TM-polarization). Therefore a negative material birefringence $\beta = (n_e - n_o)/n_o$ [11,12] is typical of Si-nc SL. In this work we confirm this theoretical prediction and report on the optical characterization and modelling of the form birefringence of Si-nc/SiO_2 superlattices. In addition we have measured that Si-nc SL show positive optical gain under high fluency pumping conditions.

2. Experimental

Waveguides were produced in a conventional evaporation system by deposition of the layered structure on a quartz substrate. Rotation of the substrate enables high deposition homogeneity over the whole wafer. More details on the growth method and apparatus are reported in Ref. [10]. Briefly, the SL structure is formed by repetitive depositions of nanometer thick SiO_y ($y \approx 1$) and SiO_2 layers. After deposition, annealing at 1100 °C in N_2 atmosphere for 1 h induces the formation of Si-nc. Table 1 reports the characteristics of the four planar waveguides (named A, B, C, D) that have been investigated. They differ mainly for the thickness of the SiO_y layers in the SL. From the transmission electron microscopy (TEM) studies it is shown that the number of periods of the SL is less than the nominal values. In fact, the annealing effect is not very efficient at the interfaces between the SL and the quartz substrate or the air when the quartz substrate is not pre-annealed to drive out residual water. Such oxidation consumes a few Si-nc/SiO_2 periods replacing them with an amorphous SiO_x layer ($x \approx 2$) where it is not possible to distinguish Si-nc and whose thickness is varying from sample to sample. Hence, the final structure of the waveguides is a sequence of four layers: a quartz cladding, a bottom SiO_x layer, a Si-nc/SiO_2 SL core layer, and a top SiO_x layer (see Fig. 1). Their thickness is determined by TEM, as reported in Table 1. By dividing the measured thickness of the SL core by the counted number of SL periods, the SL period thickness can be estimated.

To characterize the optical properties of the waveguides, standard m-line measurements have been performed with two wavelengths: $\lambda = 633$ and 543 nm. The m-line technique is a highly sensitive and accurate method to know the effective indices of the different allowed modes that can propagate in a certain planar waveguide. The position measurement of dark lines (m-lines) that appear in a laser beam reflected on the base of a prism coupled to a guide provides those values. If the core thickness and the refractive index of the substrate are known, it is in general possible to fit the effective indices having the refractive material index of the core as the only free parameter. In Fig. 2 it is possible to observe a typical m-line curve, relating to sample D.

The gain measurements were made by pumping the samples with a pulsed excitation of the third harmonic output (355 nm) of a Nd:YAG laser, operating at 10 Hz, with a pulse duration of 6 ns and a maximum average energy of 300 mJ. In addition we have measured that Si-nc SL show positive optical gain under high fluency pumping conditions [13].

3. Results and discussion

The results for each waveguide are reported in Table 2. Each point is an average of the measurements made over the whole surface of the sample. The waveguides were all single-mode waveguides.

Table 1
Nominal growth parameters and parameters extracted from cross sectional TEM images for the studied waveguides

Waveguide name	A	B	C	D
Nominal parameters				
d_{NS} (nm)	2	3	4	5
d_{SiO_2} (nm)	5	5	5	5
N_{NS}/N_{SiO_2}	45/46	45/46	45/46	45/46
TEM data				
Bottom SiO_x thickness (nm)	25	25	71	11
Superlattice thickness (nm)	152	186	214.5	295.2
Top SiO_x thickness (nm)	69.5	68	14	25
Total measured thickness (nm)	247	270	291	331

d_{NS} is the nominal thickness of the silicon oxide deposited layers, d_{SiO_2} is the nominal thickness of the silica layers, N_{Si} and N_{SiO_2} are the number of SiO and SiO_2 layers in the active superlattice.

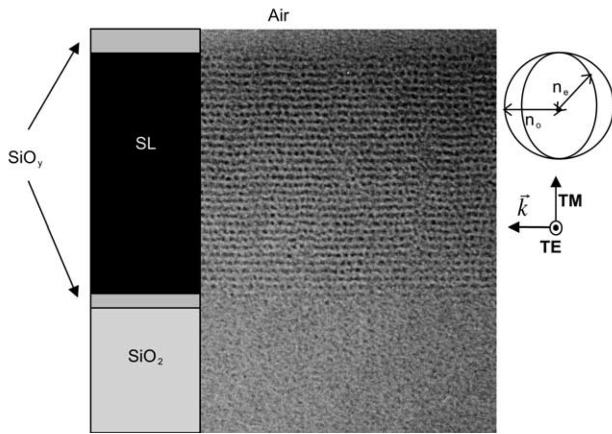

Fig. 1. TEM image of waveguide B (right) and schematization of the structure used in the simulations (left). $\vec{k}$ is the propagation vector of the guided wave. TE and TM define the two polarizations of the light. It is also shown the indices-ellipse.

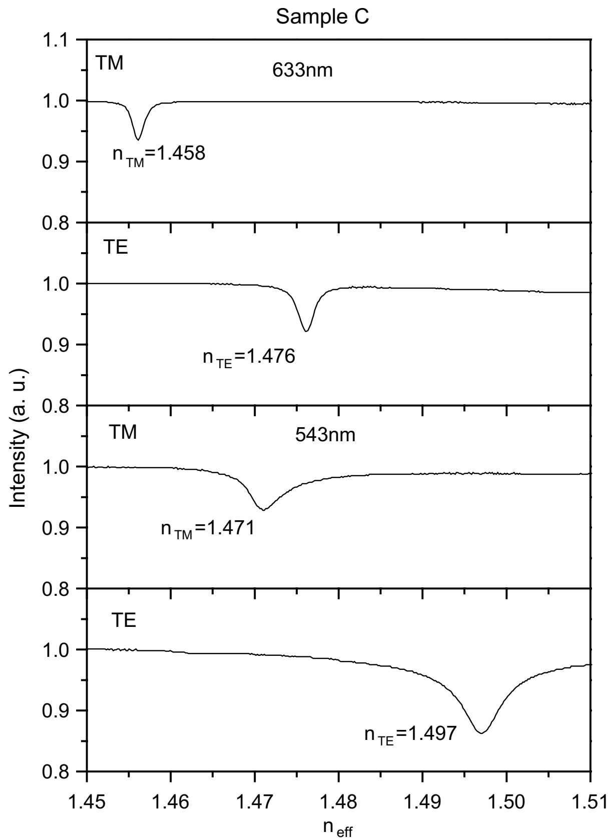

Fig. 2. M-line measurements for the TE and TM polarization on waveguide C (solid).

As expected, the effective modal indices n_{TE} and n_{TM} and the modal birefringence ($B = n_{TE} - n_{TM}$) depend on both the wavelength (due to index dispersion) and the Si-nc size (due to a variation of the overall Si content of the SL layer). Usually n_{TE} and n_{TM} can be simulated by using a waveguide simulation code, where the Si-nc rich layer is described by a single refractive index. On our data, it is impossible to fit the extracted effective indices unless we assume a different refractive index for each polarization (n_o for the ordinary and n_e for the extraordinary), therefore the structure shows a "form birefringence".

An estimation of these indices can be done by using [14,15]:

$$n_o^2 = \frac{N_{NS} n_{NS}^2 d_{NS} + N_{SiO_2} n_{SiO_2}^2 d_{SiO_2}}{d_{NS} + d_{SiO_2}} \tag{1a}$$

$$\frac{1}{n_e^2} = \frac{d_{NS} + d_{SiO_2}}{\frac{N_{NS} d_{NS}}{n_{NS}^2} + \frac{N_{SiO_2} d_{SiO_2}}{n_{SiO_2}^2}} \tag{1b}$$

where the average is performed on the SL layer assuming a periodic structure of N_{NS} layers with refractive index n_{NS} and thickness d_{NS} (the Si-nc rich layers), and N_{SiO_2} layers with a refractive index n_{SiO_2} and thickness d_{SiO_2} (the SiO_2 layers). This model fixes the condition $n_e < n_o$, i.e., negative birefringence.

One could also think that, because of the growth technique, the nanocrystals could have a preference oblate shape giving rise to a form birefringence with a different origin. However, as it can clearly be seen in the high resolution TEM micrograph of Ref. [9], statistically there is a similar number of oblong and oblate nanocrystals.

The simplest case is sample D, where we can assume a simplified waveguide structure: an air top cladding, a SiO_2 bottom cladding and a SL layer, because the number of periods in the formed SL is almost the same as its nominal value so that in the schematization of the sample we can neglect uncrystallized layers. It was assumed n_{SiO_2} to be 1.459 or 1.457 at 543 or 633 nm, respectively. Once found the ordinary (n_o) and extraordinary (n_e) refractive indices of the SL layer by simulating the m-line measurements, it is sufficient to insert their values in formulas (1a) and (1b), to obtain d_{NS}, d_{SiO_2} and n_{NS} with the only constrain that $d_{SiO_2} + d_{NS}$ should be equal to the SL period measured by TEM. In Fig. 3 we graphically show the procedure for sample D. By changing n_{NS}, and the thickness ratio ($d_{NS}/(d_{SiO_2} + d_{NS})$) only one set of parameters is compatible with the n_o and n_e deduced from the m-line measurements. This set thus fixes n_{NS}. It is interesting to note that the birefringence is maximum when the two layers have the same thickness.

In order to characterize the properties of the other waveguides the procedure has been changed slightly because of the SiO_x layers (Table 1). The refractive index of such layers is not known. But, as seen in the TEM images, no contrast between the SiO_x layers and the quartz substrate is observed, we make the conservative assumption of taking $x \approx 2$, i.e., $n_{SiO_x} \approx n_{SiO_2}$ [16]. Moreover, we will assume that the refractive index of the nanocrystal layers is independent of the sample, and we will use in the following n_{NS} as estimated for

Table 2
Summary of the different waveguide parameters extracted from the m-line measurements, simulations and TEM images

	Sample A	Waveguide B		Waveguide C		Waveguide D	
		633 nm	543 nm	633 nm	543 nm	633 nm	543 nm
n_{TE}	–	1.462 ± 0.001	1.473 ± 0.001	1.476 ± 0.001	1.497 ± 0.001	1.519 ± 0.001	1.553 ± 0.001
n_{TM}	–	1.456 ± 0.002	1.463 ± 0.001	1.458 ± 0.001	1.471 ± 0.001	1.486 ± 0.001	1.518 ± 0.001
B	–	0.006 ± 0.003	0.010 ± 0.002	0.018 ± 0.002	0.026 ± 0.002	0.033 ± 0.002	0.035 ± 0.002
Γ_{TE} (%)	–	27	42	44	59	72	81
Γ_{TM} (%)	–	3	23	10	35	56	73
n_{SiOx}	–	1.4755	1.4790	1.4755	1.4790	1.4755	1.4790
n_o	–	1.564 ± 0.003	1.568 ± 0.002	1.600 ± 0.002	1.611 ± 0.002	1.621 ± 0.001	1.643 ± 0.001
n_e	–	–	1.567 ± 0.005	1.581 ± 0.004	1.596 ± 0.002	1.603 ± 0.001	1.624 ± 0.001
β (%)	–	–	−0.5 ± 0.5	−1.1 ± 0.3	−1.0 ± 0.3	−1.1 ± 0.1	−1.1 ± 0.1
d_{NS}	–	–	2.2 ± 0.3 nm	3.1 ± 0.2 nm	3.3 ± 0.1 nm	4.4 ± 0.1 nm	4.4 ± 0.1 nm
g (cm^{-1})	−26 ± 3	27 ± 0.2		22 ± 3		−2 ± 0.5	

n_{TE} (n_{TM}) is the modal index for TE (TM) mode, $B = n_{TE} - n_{TM}$ the modal birefringence, Γ_{TE} (Γ_{TM}) the optical confinement factor in the waveguide core for TE (TM) mode, n_o and n_e the ordinary and extraordinary effective index of the core layer. $\beta = 100*(n_e - n_o)/n_o$ is the material birefringence. g is the gain coefficient at 750 nm.

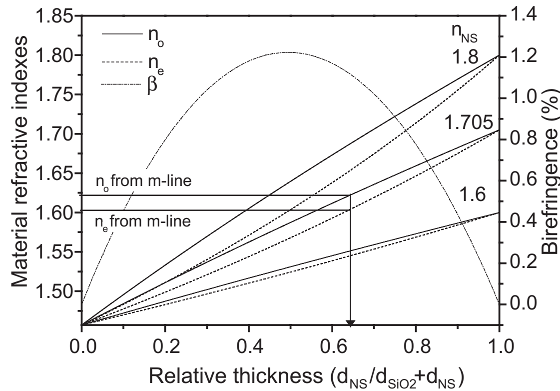

Fig. 3. Dependence of the ordinary (solid), extraordinary (dash) refractive indices with the relative thickness of the Si-nc layer that is defined as $d_{NS}/(d_{SiO_2} + d_{NS})$, for different n_{NS} refractive indices. Also shown the material birefringence (lines-dots) for $n_{NS} = 1.705$. The intersection of these curves with the vertical line is the solution of this sample, i.e., the only one that is compatible with the m-line measurement.

sample D. This is justified because the initial composition of the sub-stoichiometric layers is the same as well as the annealing temperature and procedure. In this way, a pair of n_o and n_e which fit the m-line measurements and solves Eq. (1) can be obtained with only d_{NS} and d_{SiO_2} as free parameters. In Table 2, the results of this procedure are reported. The material birefringence values we found are robust with respect to variation in n_{SiOx}.

Waveguide D has the best waveguides properties in terms of filling factors. Modelling of the structure leads to a birefringence parameter $\beta \approx -1.1\%$. n_{NS} is 1.705 at 633 nm and 1.735 at 543 nm. Waveguide C has smaller filling factors but similar $\beta \approx -1.1\%$ as waveguide D. The m-line measurement for waveguide B at 633 nm shows a weak optical confinement of the TE mode and an extremely weak one for the TM mode because of the small thickness of the SL core. No reliable birefringence value can be extracted for this wavelength. Instead, at 543 nm both TE and TM modes are confined in waveguide B. The obtained birefringence $\beta \approx -0.5\%$ is quite low comparable with the other waveguides and with the theoretical estimation. Better agreement with m-line measurements can be achieved by decreasing n_{NS} by 4% which leads to a slightly higher value of the diameter of the Si-nc than the one reported in Table 2. Sample A does not support any modes due to the significant large oxidation of the SL layers. This fact might be the main reason why this sample does not show optical gain while pumping it with high laser power.

In order to make another check of the model, we measured other Si-nc rich waveguides obtained by ion implantation and annealing [17]. By fitting the m-line measurements we found $n_o = n_e$, i.e., the core layer of the waveguides behaves as an isotropic media with refractive index in the range 1.55–1.65.

Form birefringence has been observed in many other material systems, e.g., GaAs/AlGaAs multi quantum well waveguides [15]. Due to the high refractive index contrast in the Si/SiO_2 system, the β values found in our waveguides are higher than the ones reported in the GaAs/AlGaAs system. Another silicon based material which shows a natural form birefringence is porous silicon [18,19]. Here the birefringence is due to the nature of the formation process which causes a preferential direction in the pore formation and, hence, an anisotropy in its optical properties. β values of about 10% are found for porous silicon.

It is worth noting that modelling the waveguide data yields a d_{NS} i.e., d_{NS} = 4.4, 3.3 and 2.2 nm for the D, C and B waveguide, respectively. These values are the only ones that are not depending on the used wavelength so it is a good confirmation of our procedure to reach the same values of d_{NS} with two different sets of data. These

numbers are consistent with the peak shifting of the photoluminescence spectra reported in Fig. 4 and the nominal growth parameters (Table 1).

The extracted n_{NS} value needs some comments. Its magnitude could be also evaluated by making use of the Bruggeman formula [14] for isotropic media by supposing the ideal situation in which all the Si in excess within the sub-stoichiometric layers has been consumed in the formation of silicon nanocrystals. When we do that, a Si volume fraction of 30% is obtained, which implies a $n_{NS} = 1.97$ for the red and 2.01 for the green. Taking these values of n_{NS} and using Eq. (1) we cannot reproduce the n_o and n_e values deduced by the m-line measurements. As a possible explanation we suggest that, either the composition of the matrix is not pure, or, similarly to what occurred to the top and bottom uncrystallized layers of the superlattice, not all silicon in excess is spent in the nanocrystals formation but there is the presence of amorphous SiO_x between the nanocrystals. In fact, evidences of an intermediate region of amorphous SiO_x coating the Si-nc surface have been already reported in the literature [20]. Moreover, energy filtered TEM measurements show that the quantity of Si in the Si-nc is lower than the quantity of excess Si in the deposited SiO_x [21].

We also made a study of the light emission coming from the Si-nc under the pulsed excitation of the 355 nm line of a Nd:YAG laser. The presence of high positive optical gain under high pumping energy is observed in two waveguides, which are samples B and C. This is demonstrated with a superlinear behaviour on a time resolved variable strip length measurement (TR-VSL) [23]. In Fig. 5 we show these measurements for samples A and B both at high and low pumping power, detecting at 750 nm. A very fast component lifetime (in the order of nanoseconds), that appears with rising the power, together with a threshold in the intensity of the signal, after

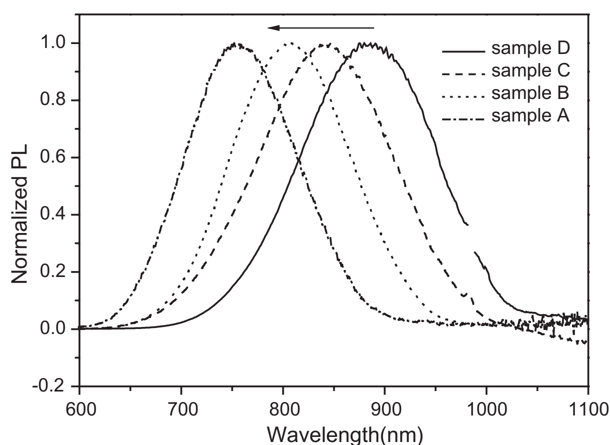

Fig. 4. Photoluminescence spectra of samples A, B, C, D while exciting the samples with the 365 nm line of an Ar laser. The spectra are normalized.

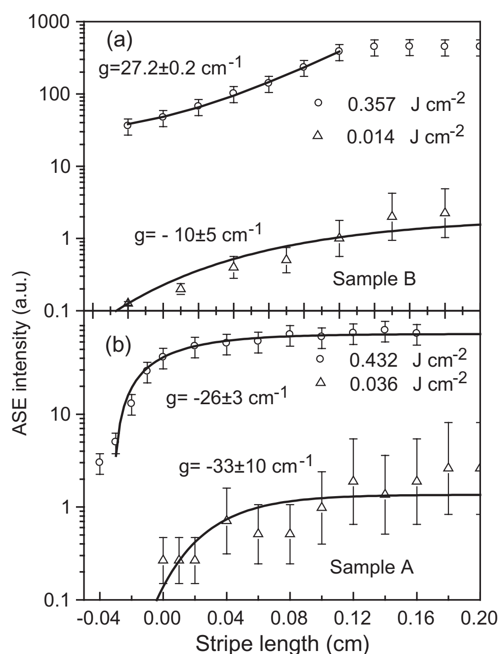

Fig. 5. (a) High (circles) and low (triangle) fluence time resolved variable stripe length (TR-VSL) data for sample B. The lines are fits to the data. The extracted gain parameters are reported. (b) The same data for the sample A. The difference in the maximum and minimum fluence employed for the two samples is due to differences in their damage thresholds. The observation wavelength was 750 nm.

what the signal grows more than linearly, are also evidences of the stimulated emission presence. These last effects become much more clear when pumping with a long stripe, because stimulated emitted light can grow up. In Table 2 the gain coefficients measured at 750 nm are reported. A more detailed analysis of the optical amplification in these samples is reported elsewhere [22]. Sample A does not show any gain because it is not acting as a waveguide. In the case of waveguide D, where the optical confinement is high, the lack of optical gain might be due to the large size of the emitting nanocrystals. There is no appreciable correlation between the presence of high material birefringence and the optical gain, but it is clear that a birefringent structure is not detrimental for the observation of optical gain. However, also because the material refractive index is lower for the TM mode, the confinement is clearly worse for this mode, therefore also the modal gain will be lower than for the TE polarized light. Measurements to check the expected result, that is higher values for the TE mode gain coefficients than the reported ones, are under way.

4. Conclusions

In conclusion, we have found a negative form birefringence of about 1% in a set of planar waveguides whose active core was a periodic repetition of a Si-nc

rich SiO_2 layer and a SiO_2 layer. This form birefringence could be exploited in optical devices such as wavelength filters, coherence modulators, polarization converter [24] and polarizing beam splitters [25]. Its modelling allows the determination of different structural and optical parameters of the superlattices. As in other reports, we found a lower Si-nc concentration than expected from pure stoichiometric arguments. We have also measured the presence of positive optical gain under pulsed excitation in two of the samples under study.

References

[1] S. Ossicini, F. Priolo, L. Pavesi, Light Emitting Silicon for Microphotonics, Springer-Verlag, New York, 2004.
[2] A. Irrera, D. Pacifici, M. Miritello, G. Franzò, F. Priolo, F. Iacona, D. Sanfilippo, G. Di Stefano, P.G. Fallica, Appl. Phys. Lett. 81 (10) (2002) 1866.
[3] G. Vijaya Prakash, M. Cazzanelli, Z. Gaburro, L. Pavesi, F. Iacona, G. Franzo, F. Priolo, J. Mod. Optics 49 (5–6) (2002) 719.
[4] L. Pavesi, L. Dal Negro, C. Mazzoleni, G. Franzò, F. Priolo, Nature 408 (2000) 440.
[5] L. Pavesi, J. Phys. Condens. Matter 15 (2003) R1169.
[6] L. Dal Negro, M. Cazzanelli, L. Pavesi, S. Ossicini, D. Pacifici, G. Franzò, F. Priolo, F. Icona, Appl. Phys. Lett. 82 (2003) 4636.
[7] L. Khriachtchev, M. Rasanen, S. Novikov, J. Sinkkonen, Appl. Phys. Lett. 79 (2001) 1249.
[8] M. Nayfeh, S. Rao, N. Barry, A. Smith, S. Chaieb, Appl. Phys. Lett. 80 (2002) 121.
[9] K. Luterova, I. Pelant, I. Mikulskas, R. Tomasiunas, D. Muller, J.J. Grob, J.L. Rehspringer, B. Hönerlage, J. Appl. Phys. 91 (2002) 2896.
[10] M. Zacharias, J. Heitmann, R. Scholz, U. Kahler, M. Schmidt, J. Bläsing, Appl. Phys. Lett. 80 (2002) 661.
[11] D. Bergman, Phys. Rep. (Sec. C of Physics Letters) 43 (9) (1978) 377.
[12] J. Kang, G.I. Stageman, C.H. Huang, D.L. Li, H.H. Lin, H.C. Chang, C.C. Yang, IEEE Photon Technol. Lett. 7 (1995) 769.
[13] L. Dal Negro, P. Bettotti, M. Cazzanelli, L. Pavesi, D. Pacifici, Optics Commun. 94 (2003) 6334.
[14] D.E. Aspnes, Am. J. Phys. 50 (8) (1982) 704.
[15] S. Ohke, T. Umeda, Y. Cho, Opt. Commun. 56 (1985) 235.
[16] S.M.A. Durrani, M.F. Al-Kuhaili, E.E. Khawaja, J. Phys. Condens. Matter 15 (2003) 8123.
[17] B. Garrido, M. López, C. Garcia, A. Pérez-Rodríguez, J.R. Morante, C. Bonafos, M. Carrada, A. Claverie, J. Appl. Phys. 91 (2002) 798.
[18] D. Kovalev, G. Polisski, J. Diener, H. Heckler, N. Kuenzner, F. Koch, Phys. Status Solidi (a) 180 (2000) R8.
[19] C.J. Oton, Z. Gaburro, M. Ghulinyan, L. Pancheri, P. Bettotti, L. Dal Negro, L. Pavesi, Appl. Phys. Lett. 81 (2002) 4919.
[20] N. Daldosso et al., Phys. Rev. B 68 (2003) 85327.
[21] F. Iacona, C. Buongiorno, C. Spinella, S. Boninelli, F. Priolo, J. Appl. Phys. 95 (2004) 3723.
[22] M. Cazzanelli et al., J. Appl. Phys. 96 (2004) 8979.
[23] K.L. Shaklee, E. Nahaory, R.F. Leheny, J. Lumin. 7 (1973) 284.
[24] Lorenzo Pavesi, David G. Lockwood, Silicon Photonics, Springer Verlag, Berlin, 2004.
[25] R.C. Tyan, P.C. Sun, Y. Fainman, Diffractive and Holographic Optics Technology III, 1996.